Electronic Structure and *g*-Factor Anisotropy of d^1 Systems in a Trigonal Environment

By **Luc G. Vanquickenborne** † and **Christiane Görller-Walrand**, Department of Chemistry, Celestijnenlaan 200F, B-3030 Heverlee, University of Leuven, Belgium
René Debuyst, Laboratoire de Chimie Inorganique et Nucleaire, 2, chemin du cyclotron, B-1348 Louvain-La-Neuve, Universite de Louvain, Belgium

The electronic structure of d^1 systems in trigonal complexes has been investigated; analytical expressions have been derived for the *g* factors in both C_{3v} (three-co-ordination) and D_{3d} (six-co-ordination) symmetry. The calculations are made on the basis of an additive point-ligand model. The angle θ between the *z* axis and the ligand bonds has been varied between 90 and 135°; the corresponding *g* values are calculated for different ligand-field parameters.

In a recent study [1] a theoretical analysis was made of the *g*-factor anisotropy of the $[CrO_3]^-$ radical ion. The ligand field affecting the central metal ion was considered to arise from a tetrahedral co-ordination sphere, where one of the ligands had been removed along the *z* axis; the resulting three-co-ordinate species (C_{3v} symmetry) was thus treated by studying the effect of a trigonal distortion of a T_d entity. The angle θ between the *z* axis and the Cr–O bonds was varied around the tetrahedral value ($\theta_t = 109.4°$) between 90 and 120° [Figure 1(*a*)].

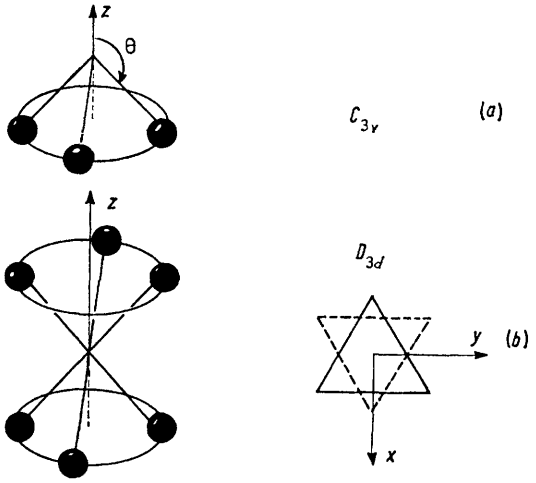

FIGURE 1 Trigonal three- and six-co-ordinate complexes. All metal–ligand distances are assumed to be equal. Symmetry: (*a*) C_{3v}, (*b*) D_{3d}

The purpose of the present investigation is two-fold. (*i*) The previous study, which was aimed specifically at an understanding of the $[CrO_3]^-$ spectrum, will be extended to accommodate a larger range of structural and chemical parameters; in this way, one might contribute to a better knowledge of three-co-ordinate d^1 species in general. (*ii*) In general, e.s.r. studies on trigonal systems make use of the crystal-field parameters B_2^0, B_4^0, and B_4, or alternatively of $10Dq$ (the cubic parameter), δ or *v* (the trigonal splitting parameter), and *v'* (the trigonal off-diagonal parameter).[2-8] The most detailed study has been carried out by Gladney and Swalen.[4] However, in their work, the systematic variation of the crystal-field parameters was not related to specific geometrical ligand rearrangements. We intend to provide a more physical understanding of the parameter variation by relating it directly to the geometrical structure of the molecule. In doing so, we will also stress the relationship between three- and six-co-ordinate complexes.

† To whom requests for reprints should be addressed.

THE LIGAND-FIELD MODEL AND THE HOLOHEDRON SYMMETRY

If the ligand field is approximated by an additive point-ligand model,[9-11] two one-electron parameters σ and π can be associated with each metal–ligand interaction [equations (1)—(5)], where $\mathscr{H}^z$ is the perturbation Hamiltonian due to

$$\sigma = E(\sigma) - E(\delta) \quad (1)$$

$$\pi = E(\pi) - E(\delta) \quad (2)$$

$$E(\sigma) = (d_{z^2}|\mathscr{H}^z|d_{z^2}) \quad (3)$$

$$E(\pi) = (d_{xz}|\mathscr{H}^z|d_{xz}) = (d_{yz}|\mathscr{H}^z|d_{yz}) \quad (4)$$

$$E(\delta) = (d_{xy}|\mathscr{H}^z)d_{xy}) = (d_{x^2-y^2}|\mathscr{H}^z|d_{x^2-y^2}) \quad (5)$$

one ligand situated on the *z* axis. In the general case, where the ligand field is composed of the contributions from the different ligands, the perturbation matrix is not diagonal in the real *d*-orbital set: the matrix elements are relatively simple functions of the (σ_L, π_L) parameters of each metal–ligand interaction, and of the angular position (θ_L, ϕ_L) of each ligand.

When two ligands L and L' are situated on the same axis on both sides of the metal ion the matrix elements are functions [9,11] of the *sums* ($\sigma_L + \sigma_L'$) and ($\pi_L + \pi_L'$); they do *not* depend on the individual parameters σ_L, σ_L', π_L, and π_L'. More specifically, whether the two ligands are identical or not has no consequence: as long as the sum $\sigma_L + \sigma_L'$ (or $\pi_L + \pi_L'$) remains constant, increasing σ_L and decreasing σ_L' does not affect the matrix elements. Therefore, the *d*-orbital perturbation matrix can exhibit a rather high effective symmetry. The structure obtained when L and L' are the same, thus effectively adding an inversion centre, is called the holohedron equivalent of the complex under consideration. The symmetry group of the actual molecule, *G*, is a subgroup of the symmetry group G_h of the holohedron.

Figure 1 shows that the trigonal three- and six-co-

ordinate structures are characterized by the same holohedron symmetry D_{3d}: the three-co-ordinate C_{3v} entity is formally unaffected by replacing the three (σ_L, π_L) ligands by three fictitious ($\sigma_L/2$, $\pi_L/2$) ligands, while at the same time adding three more fictitious ($\sigma_L/2$, $\pi_L/2$) ligands at the other side of the metal ion. The trigonal distortion of the six-co-ordinate complex is then of course described by a simultaneous change of the angles θ and $\pi - \theta$ for the upper and lower triangle respectively. The octahedron is obtained for $\theta = \frac{1}{2}\theta_t$ and $\pi - \frac{1}{2}\theta_t$; we will adopt the convention that the octahedral angle θ_0 is given by $(\pi - \frac{1}{2}\theta_t) = 125.3°$.

In what follows, we restrict our attention to a trigonal distortion, which is completely described by angular variations, *i.e.* the metal–ligand distances are assumed to remain constant. This restriction will allow us to carry out the analysis by means of only two orbital parameters, σ and π.

The non-zero elements of the perturbation matrix as a function of θ are given by equations (6)—(9) where $N = 3$ or 6 (the number of identical ligands). If we define [1,12] the expressions in (10) and (11), the e levels are described by the following wavefunctions and energies:

$$E(z^2) = (z^2|\mathscr{H}|z^2) = N[\tfrac{1}{4}(3\cos^2\theta - 1)^2\sigma + (3\cos^2\theta\sin^2\theta)\pi] \quad (6)$$

$$H_{AA} = (yz|\mathscr{H}|yz) = (xz|\mathscr{H}|xz) = N[\tfrac{3}{8}(\sin^2 2\theta)\sigma + \tfrac{1}{2}(\cos^2\theta + \cos^2 2\theta)\pi] \quad (7)$$

$$H_{BB} = (xy|\mathscr{H}|xy) = (x^2 - y^2|\mathscr{H}|x^2 - y^2) = N[\tfrac{3}{8}(\sin^4\theta)\sigma + \tfrac{1}{2}(\sin^2\theta + \tfrac{1}{4}\sin^2 2\theta)\pi] \quad (8)$$

$$H_{AB} = (yz|\mathscr{H}|xy) = -(xz|\mathscr{H}|x^2 - y^2) = -\frac{N}{4}\cos\theta\sin^3\theta(3\sigma - 4\pi) \quad (9)$$

$$\tan 2\alpha = 2H_{AB}/(H_{AA} - H_{BB}) \text{ where } \frac{\pi}{2} \leqslant 2\alpha \leqslant \frac{3\pi}{2} \quad (10)$$

$$\xi = \alpha \text{ for } H_{AA} \leqslant H_{BB},$$

$$\text{while} \quad \xi = \alpha + \frac{\pi}{2} \text{ for } H_{AA} > H_{BB} \quad (11)$$

$$E_- = H_{AA} - H_{AB}\text{cotan}\,\xi \quad (12)$$

$$|\psi_-\rangle = \sin\xi|yz\rangle - \cos\xi|xy\rangle \quad (13)$$

$$|\psi_-'\rangle = \sin\xi|xz\rangle + \cos\xi|x^2 - y^2\rangle \quad (14)$$

$$E_+ = H_{BB} + H_{AB}\text{cotan}\,\xi \quad (15)$$

$$|\psi_+\rangle = \cos\xi|yz\rangle + \sin\xi|xy\rangle \quad (16)$$

$$|\psi_+'\rangle = \cos\xi|xz\rangle - \sin\xi|x^2 - y^2\rangle \quad (17)$$

With the conventions as specified, H_{AB}cotan ξ is always positive and E_- is the energy of the lowest e level and E_+ the energy of the highest e level, irrespective of the relative values of H_{AA} and H_{BB}.

In our previous work the σ and π parameters were appropriate for the $[CrO_3]^-$ ion:[1,13] $\sigma = 13\,900$ cm^{-1} and $\pi = 3\,880$ cm^{-1}. From a number of ligand-field studies,[9,10,14] the quotient π/σ, being a measure of the relative π- and σ-bonding capabilities, varies for most ligands (except possibly for certain π acceptors) and metals, from 0 (for pure σ donors) to *ca.* 0.3 (for strong π donors). Figure 2 shows a few typical examples from a series of calculations where σ was varied from 4 000 to 16 000 cm^{-1} and π/σ from 0 to 0.5.

The ($\theta = 90°$) case corresponds to the planar D_{6h} holohedron, and the diagonal elements are given by $H_{AA} = N(\frac{1}{2}\pi)$ and $H_{BB} = N\left(\frac{3}{8}\sigma + \frac{\pi}{2}\right)$. Therefore, at $\theta = 90°$, $H_{AA} < H_{BB}$. At the right-hand side of the diagram, where $\theta = 135°$, the diagonal elements are given by $H_{AA} = N(\frac{3}{8}\sigma + \frac{1}{4}\pi)$ and $H_{BB} = N(\frac{3}{32}\sigma + \frac{3}{8}\pi)$; hence, here $H_{AA} > H_{BB}$. Therefore H_{AA} and H_{BB} will always cross in the relevant θ range; their crossing point will be denoted θ'. $|H_{AB}|$ on the other hand starts at zero when $\theta = 90°$, reaches a maximum at $\theta = 120°$, and then decreases again. This means that in the region where H_{AA} and H_{BB} approach each other $|H_{AB}|$ will reach its maximal value, thereby repelling the two e levels in a very effective way. Therefore, the two e levels will remain rather far apart throughout the whole diagram.

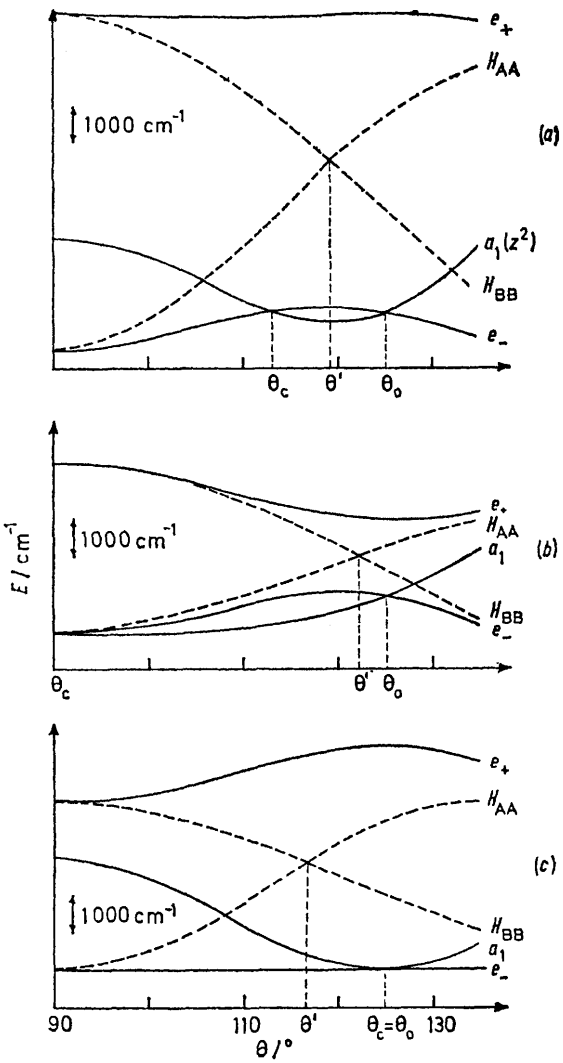

FIGURE 2 Orbital-energy diagrams as a function of the geometrical distortion angle θ (defined in Figure 1): (*a*) $\pi/\sigma = 0.25$, $\sigma = 8\,000$ cm^{-1}; (*b*) $\pi/\sigma = 0.5$, $\sigma = 4\,000$ cm^{-1}; (*c*) $\pi/\sigma = 0$, $\sigma = 4\,000$ cm^{-1}

At $\theta = \theta_0 = 125.3°$ the holohedron is octahedral and the

lowest level should be three-fold degenerate; this means that E_- and $E(z^2)$ should intersect at $\theta = \theta_0$. In Figure 2(*a*) it is obvious that a second intersection occurs at θ_c situated between 90 and 125.3°. In Figure 2(*b*) the second intersection is at 90°, while in Figure 2(*c*) the second intersection is coincident with $\theta = \theta_0$; indeed, if $\pi = 0$, the extremum of z^2 is situated at $\cos^2\theta = (\sigma - 2\pi)/(3\sigma - 4\pi) = \frac{1}{3}$, that is at $\theta = \theta_0$.

The evolution of ξ as a function of θ (Figure 2) is completely described by equations (10)—(17). If $\theta = 90°$, $\xi = \alpha = 90°$; if θ increases $\xi = \alpha$ decreases monotonously and reaches the value 45° at θ'. At this point ξ jumps abruptly to reach the value $\xi = \alpha + 90° = 225°$ and then continues to decrease regularly (at $\theta = \theta_0$, $\xi = \theta_0 + 90°$).

In the θ range under consideration the difference between the two lowest-energy levels is rather small, while the highest *e* level is at relatively high energy. Therefore, the effect of spin–orbit interaction will be restricted to the lowest subset of two energy levels. The spin functions (α, β) form a basis for Γ_4^+ in D_{3d}; therefore the a_1 level becomes $\Gamma_1^+ \times \Gamma_4^+ = \Gamma_4^+$, while the *e* levels give rise to $\Gamma_3^+ \times \Gamma_4^+ = \Gamma_4^+ + \Gamma_5^+ + \Gamma_6^+$. The Γ_4^+ orbitals interacting under the influence of spin–orbit coupling are given by (18) where the *d* orbitals $|0\rangle$, $|\pm1\rangle$, $|\pm2\rangle$ satisfy the

$$\left.\begin{aligned} a_1(\Gamma_4^+)&\left\{\begin{aligned}&|0\alpha\rangle\\&|0\beta\rangle\end{aligned}\right.\\ e(\Gamma_4^-)&\left\{\begin{aligned}|e_-\beta\rangle &= -2^{-\frac{1}{2}}[|\psi_-'\beta\rangle + \mathrm{i}|\psi_-\beta\rangle]\\ &= \sin\xi|1,\beta\rangle - \cos\xi|-2,\beta\rangle\\ |e_-'\alpha\rangle &= 2^{-\frac{1}{2}}[|\psi_-'\alpha\rangle - \mathrm{i}|\psi_-\alpha\rangle]\\ &= \sin\xi|-1,\alpha\rangle + \cos\xi|2,\alpha\rangle\end{aligned}\right.\end{aligned}\right\} \quad (18)$$

Condon–Shortley sign convention. The (Γ_5^+, Γ_6^+) level is described by (19) and (20).

$$\begin{aligned}|e_-\alpha\rangle &= -2^{-\frac{1}{2}}[|\psi_-'\alpha\rangle + \mathrm{i}|\psi_-\alpha\rangle]\\ &= \sin\xi|1,\alpha\rangle - \cos\xi|-2,\alpha\rangle \quad (19)\end{aligned}$$

$$\begin{aligned}|e_-'\beta\rangle &= 2^{-\frac{1}{2}}[|\psi_-'\beta\rangle - \mathrm{i}|\psi_-\beta\rangle]\\ &= \sin\xi|-1,\beta\rangle + \cos\xi|2,\beta\rangle \quad (20)\end{aligned}$$

The first-order splitting of the e_- level is given by $E(\Gamma_4 e) - E(\Gamma_5, \Gamma_6) = (3\cos^2\xi - 1)\zeta$ where ζ is the spin–orbit coupling constant of the metal. It follows that $\Gamma_{5,6}$ is the lowest *e* component if $|H_{AB}/(H_{AA} - H_{BB})| > 2^{\frac{1}{2}}$. This is always the case when $H_{AA} > H_{BB}$; it is also true when $H_{AA} < H_{BB}$, if $H_{AA} - H_{BB}$ is very small, that is in the immediate neighbourhood of the crossing point θ'. In the other cases Γ_4 is the lowest *e* component (Figure 3).

This pattern is of course thoroughly modified by the off-diagonal elements of the spin–orbit coupling operator.

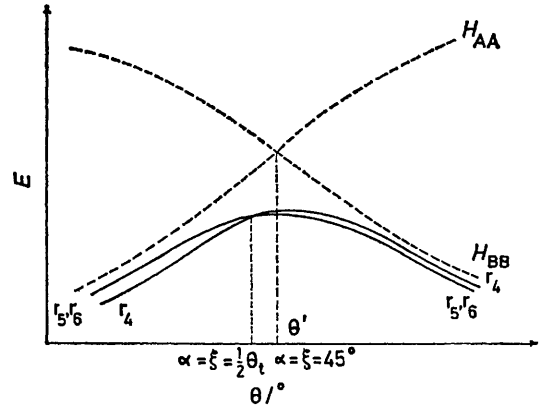

FIGURE 3 Schematic energy-level diagram of the first-order spin–orbit splitting of a hypothetically isolated e_- level in D_{3d} as a function of θ

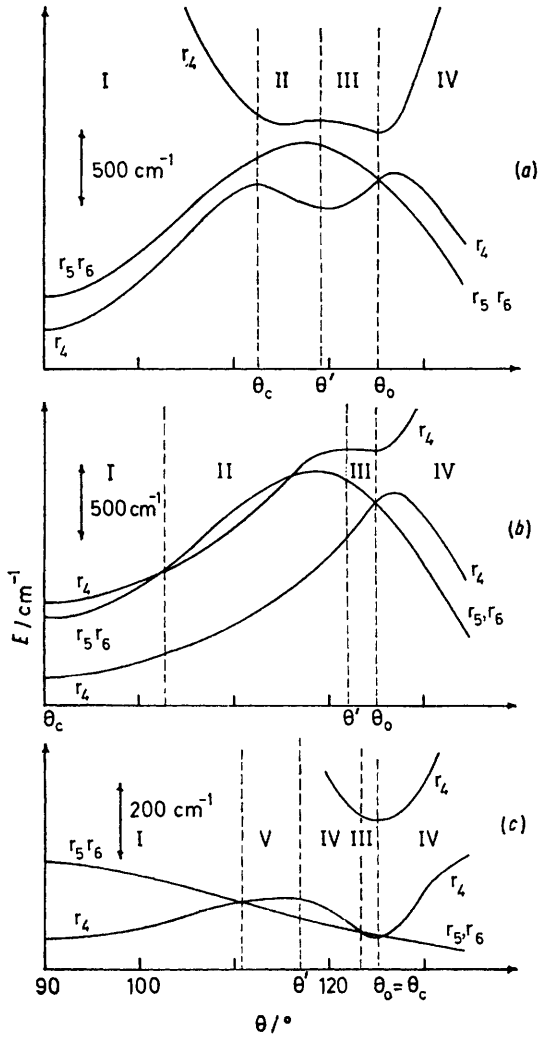

FIGURE 4 Energy-level diagram (including spin–orbit coupling) of a d^1 D_{3d} entity as a function of θ; the zone labels I through V are defined in the text (ζ = 200 cm^{-1})

Defining the expressions (21) and (22), with $90 \leqslant 2\gamma \leqslant 270°$; let $\eta = \gamma$ if $\Delta E \geqslant 0$, $\eta = \gamma + 90°$ if $\Delta E < 0$, then

$$\begin{aligned}\Delta E &= E(z^2) - E(\Gamma_4 e)\\ &= E(z^2) - E(e_-) - \tfrac{1}{2}(3\cos^2\xi - 1)\zeta \quad (21)\end{aligned}$$

$$\tan 2\gamma = \zeta 6^{\frac{1}{2}} \sin\xi/\Delta E \quad (22)$$

the resulting wavefunctions of the lowest Γ_4 state are given by (23) and (24).

$$|k\rangle = \sin\eta|e_-'\alpha\rangle + \cos\eta|0\beta\rangle \quad (23)$$

$$|k'\rangle = \sin\eta|e_-\beta\rangle + \cos\eta|0\alpha\rangle \quad (24)$$

From Figure 2 it is clear that the $a_1(z^2)$ orbital intersects the e_- level in the neighbourhood of θ'. The avoided crossings and the energy shifts due to the off-diagonal matrix elements of the spin–orbit coupling operator transform Figures 2 and 3 into 4.

g FACTORS AND DISCUSSION OF THE RESULTS

In order to analyse the evolution of the *g* factors as a function of θ it is useful to distinguish different regions in Figure 4. In principle, eight different regions are

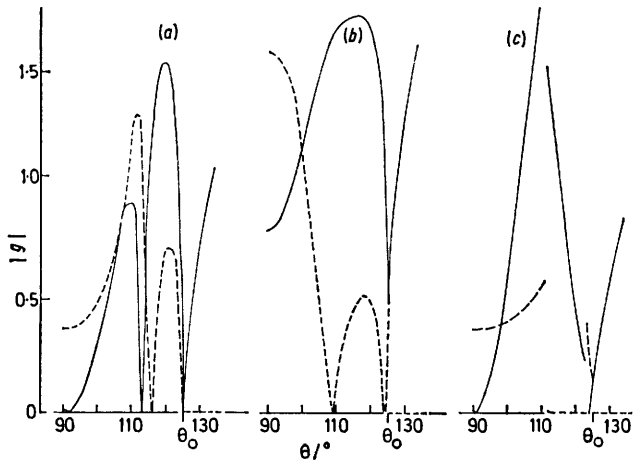

FIGURE 5 Variation of the *g* factors as a function of θ ($\zeta = 200$ cm^{-1}): (*a*) $\sigma = 8\,000$, $\pi = 2\,000$; (*b*) $\sigma = 4\,000$, $\pi = 2\,000$; (*c*) $\sigma = 4\,000$ cm^{-1}, $\pi = 0$ cm^{-1}: (——) $g_{\|}$, (— — —) $g_{\perp}$

possible: the ground state can be either Γ_4 or (Γ_5, Γ_6); in both cases $H_{AA} \gtrless H_{BB}$ and $E \gtrless 0$. In Figure 4, only five regions are to be considered. If the ground state as Γ_4 symmetry three possibilities arise:

I $H_{AA} \leqslant H_{BB}$; $\Delta E \geqslant 0$ $\xi = \alpha$; $\eta = \gamma$

II $H_{AA} \leqslant H_{BB}$; $\Delta E < 0$ $\xi = \alpha$; $\eta = \gamma + 90°$

III $H_{AA} > H_{BB}$; $\Delta E < 0$ $\xi = \alpha + 90°$; $\eta = \gamma + 90°$

If the ground state has (Γ_5, Γ_6) symmetry two possibilities are to be considered:

IV $H_{AA} > H_{BB}$; $\Delta E \geqslant 0$ $\Delta W > 0$
$\xi = \alpha + 90°$; $\eta = \gamma$

V $H_{AA} \leqslant H_{BB}$; $\Delta E \geqslant 0$ $\Delta W > 0$
$\xi = \alpha$; $\eta = \gamma$

The corresponding *g* factors are immediately calculated from equations (19), (20), (23), and (24). Thus, for I—III we obtain (25) and (26), and for IV and V we

$$|g_{\perp}| = 2|\cos^2\eta - 3\cos^2\xi\sin^2\eta| \quad (25)$$

$$|g_{\|}| = 2|\cos^2\eta + 6^{\frac{1}{2}}\sin\xi\sin\eta\cos\eta| \quad (26)$$

obtain (27) and (28). Figure 5 shows the variation of

$$|g_{\|}| = 2|2 - 3\cos^2\xi| \quad (27)$$

$$g_{\perp} = 0 \quad (28)$$

$|g_{\|}|$ and $|g_{\perp}|$ as a function of θ.

First, it should be stressed that the results of Figure 5 (as well as Figures 4 and 6) are obtained from a computer diagonalization of the *complete d*-orbital set (thus including the higher e_+ level). Quantitatively, the computer results usually differ in the second decimal place from the analytical values. Yet, the general trends of the curves are very well reproduced by the analytical formulae (25)—(28), thereby providing an *a posteriori* justification for the neglect of the upper e_+ level in a qualitative treatment of the *g*-factor anisotropy. It is obvious from Figure 5, and implicit in equations (25)—(28), that the *g* factors are extremely sensitive functions of the distortion angle θ. In the entire range of θ values, both $g_{\|}$ and $g_{\perp}$ remain well below the spin-only value; that is, the orbital contribution to the molecular magnetic moment is always quite significant.

Comparison between experimental data and the theoretical values, as reproduced in Figure 5, can be useful in identifying certain paramagnetic species. In order to make a full comparison between theory and experiment, one needs e.s.r. data, optical spectra, as well as an *X*-ray structure analysis. An example of a combination of these data can be found in ref. 1; in most cases, however, it is difficult to obtain a complete set of experimental data.

Figure 6 shows that the qualitative features of the *g*-factor evolution are maintained when the value of the spin–orbit coupling constant is modified from 200 to 500 cm^{-1}.

It is well to notice that the *g* tensor becomes isotropic for $\theta = \theta_0$. In this case, the analytical formulae (25)—(28) are not valid; instead, one has to consider the

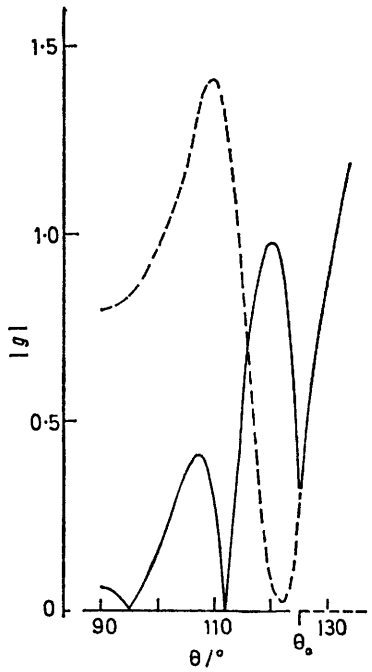

FIGURE 6 Variation of the *g* factors as a function of θ ($\zeta = 500$ cm^{-1}, $\sigma = 8\,000$ cm^{-1}, $\pi = 2\,000$ cm^{-1}): (——) $g_{\|}$, (— — —) $g_{\perp}$

splitting pattern corresponding to the four-fold degenerate Γ_8 cubic level [15] [equation (29)].

$$g_{\|} = g_{\perp} = 4\zeta/(3\sigma - 4\pi) \quad (29)$$

In the Ligand Field section we emphasized the formal identity of D_{3d} holohedrons, irrespective of the co-

ordination numbers ($N = 3$ or 6). This means that the ligand-field diagrams (Figure 2) for $N = 3$ or 6 are exactly identical except for a scaling factor of 2. If spin–orbit coupling is included, however (Figures 3 and 4), the diagrams remain identical only if ζ is simultaneously modified by a factor of 2. In that case, the g factors are independent of N.

The trigonal distortion of octahedral d^1 systems has been treated in standard texts.[2,3] For example, in the analysis of the Ti^{3+} ion the trigonal splitting δ of the cubic t_{2g} level can be introduced as a parameter. However, the authors [2,3] continue their analysis in the hypothesis that the trigonal field does not mix significantly the t_{2g} and e_g levels. Therefore, they use the *cubic* wavefunctions in deriving the g factors; this means that the mixing coefficients in equations (12)—(17) are taken to be $\pm(1/3)^{\frac{1}{2}}$ and $\pm(2/3)^{\frac{1}{2}}$, instead of $\pm\sin\xi$ and $\pm\cos\xi$. On the basis of this hypothesis, one obtains [2] expressions (30) and (31).

$$g_{\parallel} = \frac{3(\zeta + 2\delta)}{[(\zeta + 2\delta)^2 + 8\zeta^2]^{\frac{1}{2}}} - 1 \qquad (30)$$

$$g_{\perp} = \frac{\zeta}{[(\zeta + 2\delta)^2 + 8\zeta^2]^{\frac{1}{2}}} + 1 \qquad (31)$$

If we consider, for example, a trigonal distortion corresponding to $\theta = 120°$ (as compared to the cubic value of 125.3°), equations (10)—(17) predict $\delta = 820$ cm^{-1} (for $\sigma = 8\,000$ cm^{-1} and $\pi = 2\,000$ cm^{-1}). With $\zeta = 200$ cm^{-1}, equations (30) and (31) yield $g_{\parallel} = 1.87$ and $g_{\perp} = 1.10$. If on the other hand one uses equations (25) and (26), the results are $g_{\parallel} = 1.79$ and $g_{\perp} = 1.25$. The discrepancy is significant; we conclude that second-order effects of e_+ should be taken into account, certainly for the trigonal field and perhaps even for spin–orbit coupling. It appears to be a doubtful procedure to introduce covalency effects and orbital-reduction factors k (or even $k_{\parallel}$ and $k_{\perp}$) *before* allowing for all the consequences inherent in the ligand-field picture. Although this point has already been made emphatically by Gladney and Swalen,[4] even the recent literature contains many examples where orbital-reduction factors are introduced in a rather uncritical way.

One of us (R. D.) is indebted to the F.N.R.S. Belgium for support.

[8/1023 *Received*, 1*st June*, 1978]

REFERENCES

[1] L. G. Vanquickenborne, C. Görller-Walrand, and R. Debuyst, *J. Magnetic Resonance*, 1978, **29**, 275.
[2] A. Carrington and A. D. McLachlan, 'Introduction to Magnetic Resonance,' Harper, New York, 1967.
[3] A. Abragam and B. Bleany, 'Electronc Paramagnetic Resonance of Transition Ions,' Clarendon Press, Oxford, 1970.
[4] H. M. Gladney and J. D. Swalen, *J. Chem. Phys.*, 1965, **42**, 1999.
[5] N. Rumin, C. Vincent, and D. Walsh, *Phys. Rev.*, 1973, **B7**, 1811.
[6] Whei-Lu Kwik and E. I. Stiefel, *Inorg. Chem.*, 1973, **12**, 2337.
[7] H. F. Mollet and B. C. Gerstein, *J. Chem. Phys.*, 1974, **60**, 1440.
[8] P. I. Premoviç and P. R. West, *Canad. J. Chem.*, 1975, **53**, 1630.
[9] L. G. Vanquickenborne and A. Ceulemans, *J. Amer. Chem. Soc.*, 1977, **99**, 2208.
[10] L. G. Vanquickenborne, J. Vranckx, and C. Görller-Walrand, *J. Amer. Chem. Soc.*, 1974, **96**, 4121.
[11] C. E. Schäffer, *Structure and Bonding*, 1972, **14**, 69.
[12] S. P. McGlynn, L. G. Vanquickenborne, M. Kinoshita, and D. G. Carroll, 'Introduction to Applied Quantum Chemistry,' Holt, Rinehart, and Winston, New York, 1972.
[13] L. DiSipio, L. Oleari, and P. Day, *J.C.S. Faraday II*, 1972, 776.
[14] C. Görller-Walrand, J. Peeters, and L. Vanquickenborne, *J. Chim. phys.*, 1974, **71**, 633.
[15] C. Ballhausen, 'Introduction to Ligand Field Theory,' McGraw-Hill, New York, 1962.